nature cell biology

STIM1 carboxyl-terminus activates native SOC, I_{crac} and TRPC1 channels

Guo N. Huang[1,2,5], Weizhong Zeng[3,5], Joo Young Kim[3], Joseph P. Yuan[3], Linhuang Han[1], Shmuel Muallem[3,6] and Paul F. Worley[1,4,6]

Receptor-evoked Ca^{2+} signalling involves Ca^{2+} release from the endoplasmic reticulum, followed by Ca^{2+} influx across the plasma membrane[1]. Ca^{2+} influx is essential for many cellular functions, from secretion to transcription, and is mediated by Ca^{2+}-release activated Ca^{2+} (I_{crac}) channels and store-operated calcium entry (SOC) channels[2]. Although the molecular identity and regulation of I_{crac} and SOC channels have not been precisely determined[1], notable recent findings are the identification of STIM1, which has been indicated to regulate SOC and I_{crac} channels by functioning as an endoplasmic reticulum Ca^{2+} sensor[3–6], and ORAI1 (ref. 7) or CRACM1 (ref. 8) — both of which may function as I_{crac} channels or as an I_{crac} subunit. How STIM1 activates the Ca^{2+} influx channels and whether STIM1 contributes to the channel pore remains unknown. Here, we identify the structural features that are essential for STIM1-dependent activation of SOC and I_{crac} channels, and demonstrate that they are identical to those involved in the binding and activation of TRPC1. Notably, the cytosolic carboxyl terminus of STIM1 is sufficient to activate SOC, I_{crac} and TRPC1 channels even when native STIM1 is depleted by small interfering RNA. Activity of STIM1 requires an ERM domain, which mediates the selective binding of STIM1 to TRPC1, 2 and 4, but not to TRPC3, 6 or 7, and a cationic lysine-rich region, which is essential for gating of TRPC1. Deletion of either region in the constitutively active $STIM1^{D76A}$ yields dominant-negative mutants that block native SOC channels, expressed TRPC1 in HEK293 cells and I_{crac} in Jurkat cells. These observations implicate STIM1 as a key regulator of activity rather than a channel component, and reveal similar regulation of SOC, I_{crac} and TRPC channel activation by STIM1.

Receptor and SOC channels are essential for the maintenance of Ca^{2+} stores within the endoplasmic reticulum at precise levels — for signalling in both non-excitable and excitable tissues, and for the mediation of diverse cellular functions[1,2]. One form of SOC is the I_{crac} channel. The molecular identity of SOC and I_{crac} channels are not known, although several studies implicate members of the canonical transient receptor potential (TRPC) subfamily of TRP channels in SOC-channel activity[1]. Recently, STIM1 was identified in screens for molecules that are essential for the activation of SOC and I_{crac} channels[5,6]. STIM1 possesses a signal sequence and a single transmembrane domain, indicating a topology that places an EF-hand domain either within the lumen of the endoplasmic reticulum or exposed on the plasma membrane[5,6,9] (Fig. 1a). Mutation of the EF hand results in constitutively active STIM1 (refs 3, 4, 6), and increases its localization near or at the plasma membrane[4,6]. To examine the molecular basis of STIM1 function, we established a screening assay based on the translocation of a transcription factor, nuclear factor of activated T cells (NFAT), to the nucleus in response to sustained elevation of cytoplasmic Ca^{2+} (ref. 10). As expected, NFAT–GFP localizes to the cytoplasm in resting HEK cells (Fig. 1b and see Supplementary Information, Fig. S1). When Ca^{2+} entry is increased, consequent to depletion of the endoplasmic reticulum Ca^{2+} store by either ionomycin or a sarco/endoplasmic reticulum Ca^{2+} ATPase (SERCA) Ca^{2+} pump blocker (thapsigargin), NFAT–GFP translocates into the nucleus. Nuclear localization is calcineurin-dependent as it is blocked by FK506 (Fig. 1b). When wild-type STIM1 is cotransfected with NFAT–GFP into HEK cells, NFAT–GFP remains in the cytoplasm (Fig. 1b). In contrast, the constitutively active mutant $STIM1^{D76A}$ (ref. 6) induces the accumulation of NFAT–GFP in the nucleus, and this is blocked by FK506 or by a SOC-channel blocker SKF96365 (Fig. 1b).

Using the NFAT nuclear-localization assay, we examined the structure–function properties of STIM1. The cytosolic carboxyl terminus of STIM1 ($STIM1^{CT}$), which lacks a transmembrane domain, induces NFAT localization to the nucleus in the absence of Ca^{2+} store depletion (Fig. 1c). The $STIM1^{CT}$ contains several discrete regions: a conserved ERM (ezrin/radixin/moesin) domain (see Supplementary Information, Fig. S2), a glutamate-rich region, a serine–proline-rich

[1]Department of Neuroscience, [2]Program in Biochemistry, Cellular and Molecular Biology, The Johns Hopkins University School of Medicine, Baltimore, MD 21205, USA. [3]Department of Physiology, University of Texas Southwestern Medical Center, Dallas, TX 75390, USA. [4]Department of Neurology, The Johns Hopkins University School of Medicine, Baltimore, MD 21205, USA.
[5]These authors contributed equally to this work.
[6]Correspondence should be addressed to S.M. or P.F.W. (e-mail: Shmuel.muallem@utsouthwestern.edu; pworley@jhmi.edu)

Received 12 April 2006; accepted 12 June 2006; published online 13 August 2006; DOI: 10.1038/ncb1454

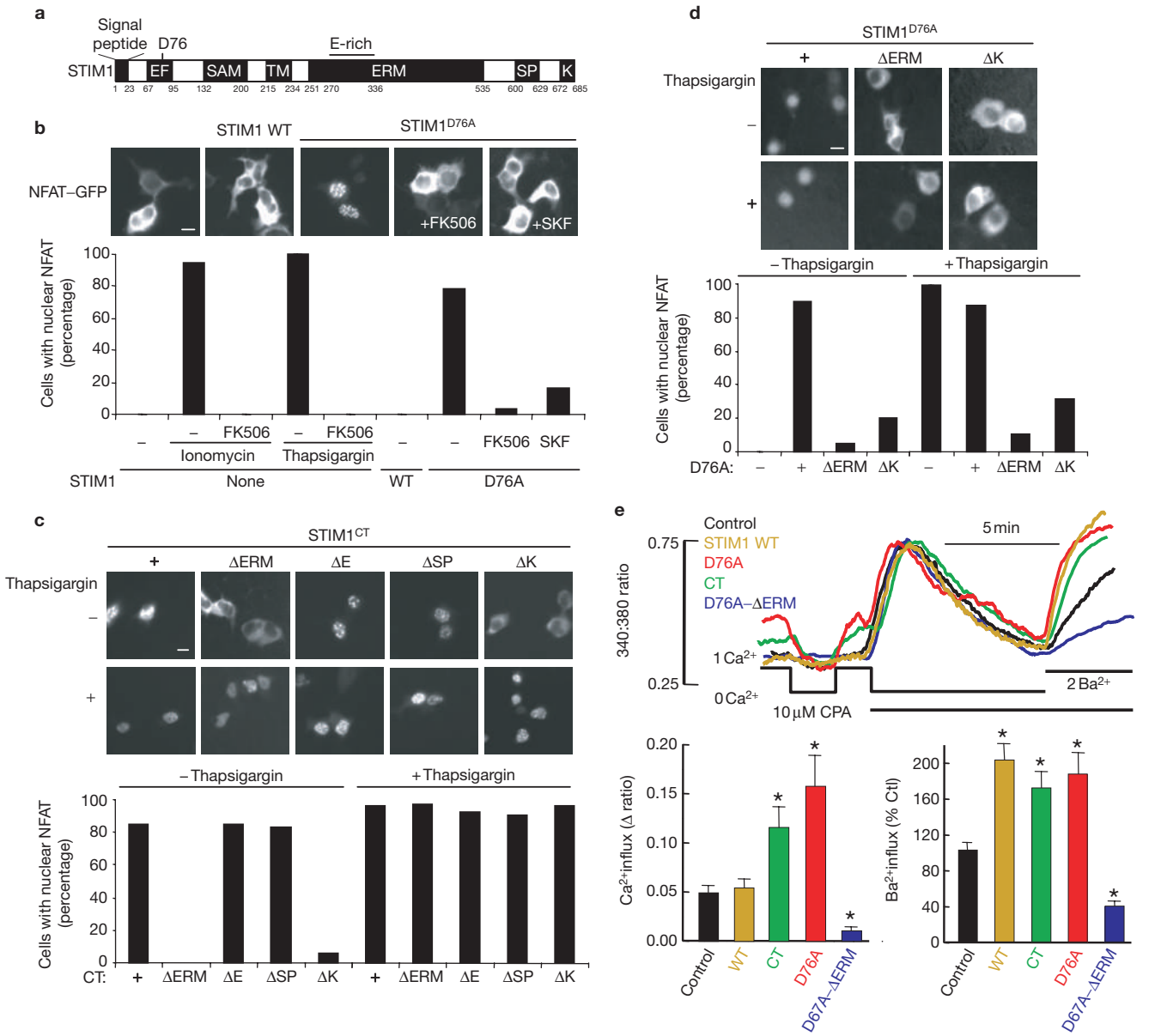

Figure 1 The EF-hand mutant and cytosolic fragment of STIM1 activate endogenous SOC channels in HEK293 cells. (**a**) Schematic representation of human STIM1 domain structure. The conserved D76 in the EF hand is shown. (**b**) Representative live images of HEK293 cells expressing NFAT1–GFP and the indicated full-length STIM1 proteins in the presence of indicated drugs. Below is the summary of all data quantifying the percentage of cells with nuclear NFAT. WT, wild type. (**c**) Images of NFAT1–GFP in cells coexpressing the indicated wild-type or deletion mutants of STIM1 cytosolic termini. The cells were imaged and scored before (–) or after (+) thapsigargin (thap) treatment, and the summary data is shown below. (**d**) The effect of thapsigargin treatment on NFAT1–GFP localization when coexpressed with $STIM1^{D76A}$ full-length or mutants lacking either the ERM domain or the lysine-rich tail. The scale bars represent 10 μm in **b**–**d**. Values are the means of scoring results of three wells with at least 100 cells counted per well. (**e**) HEK293 cells expressing empty vector (control) or the indicated STIM1 constructs and bathed in medium containing 1 mM Ca^{2+} were perfused with Ca^{2+}-free medium and then with media containing 1 mM Ca^{2+}. The extent of change in 340:380 Fura 2 ratio measured after 2 min of incubation in Ca^{2+}-free media is indicative of the cell permeability to Ca^{2+}. Results from 4–7 experiments are plotted in the columns. The cells were then incubated in Ca^{2+}-free medium containing 10 μM cyclopiazonic acid (CPA) to deplete the stores and divalent cation permeability was determined from the rate of Ba^{2+} influx, which was determined from the first derivative of the Ba^{2+} influx traces. All results are the mean ± s.e.m. (Control, $n=7$; CT, $n=7$; D76A, $n=6$; D76A–ΔERM, $n=6$; WT, $n=4$). * donates $P < 0.05$ relative to control cells transfected with empty vector.

region and a lysine-rich region. To identify regions that are important for SOC-channel activation, we deleted each region separately, and found that $STIM1^{CT}$ mutants lacking either the ERM domain or the lysine-rich region lose the ability to drive GFP–NFAT into the nucleus (Fig. 1c). Furthermore, $STIM1^{D76A}$ full-length mutants lacking either the ERM domain or the lysine-rich region do not induce nuclear translocation of NFAT, and block GFP–NFAT translocation after store depletion by thapsigargin in >90% and 70% of the cells, respectively, indicating that they act as dominant-negatives (Fig. 1d). In contrast, wild-type STIM1 lacking the ERM domain or the lysine-rich region are less effective dominant-negatives that block store-depletion-dependent NFAT translocation in 50% and 40% of cells, respectively (data not shown). These findings reveal the importance of both the ERM domain and the lysine-rich tail of STIM1 in activating endogenous SOC channels.

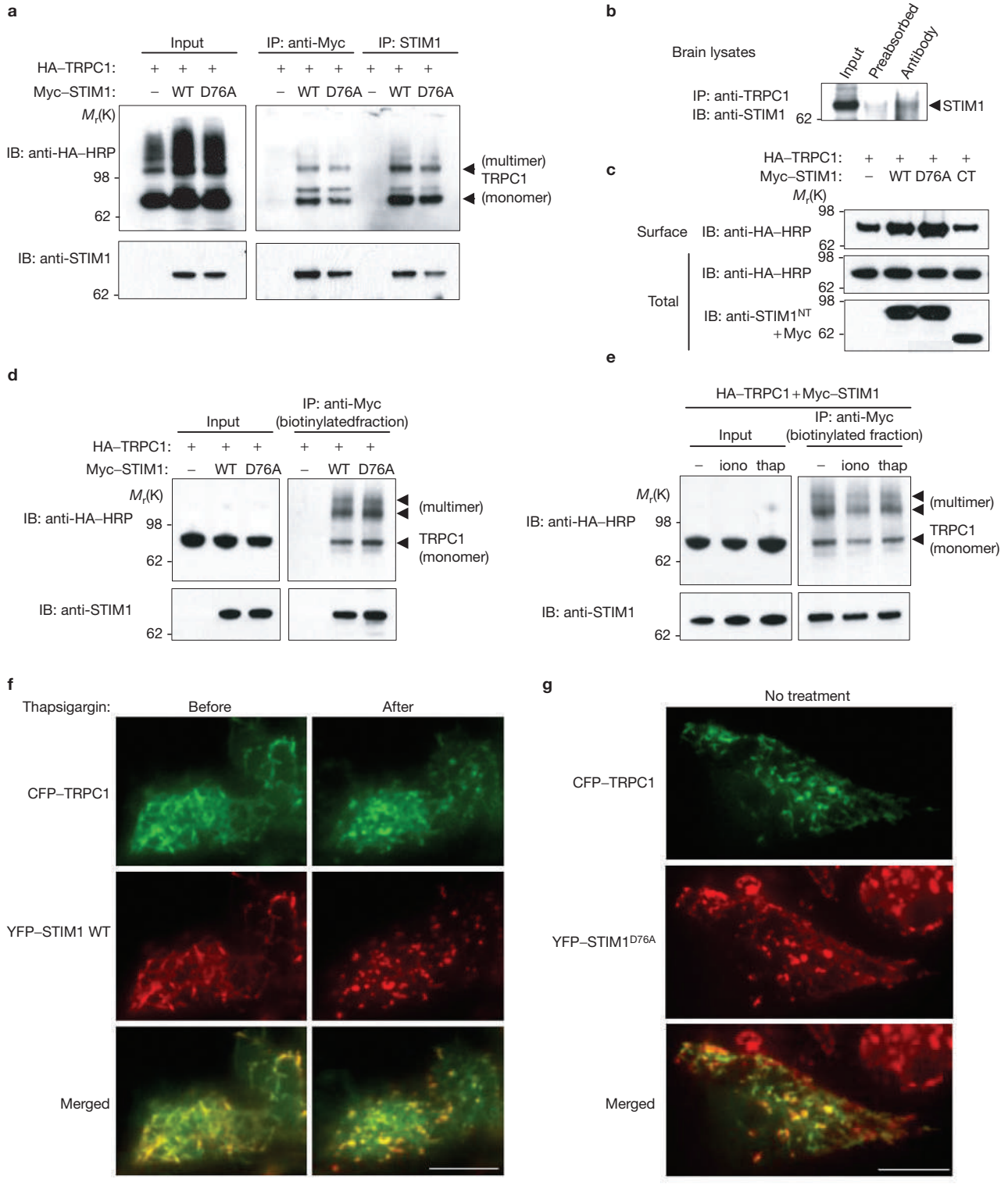

Figure 2 STIM1 and TRPC1 interaction and punctae formation. (**a**) Coimmunoprecipitation of TRPC1 and wild-type (WT) or active STIM1 from HEK293 cells. IB, immunoblot. (**b**) Endogenous TRPC1 and STIM1 coimmunoprecipitation. Brain lysates were immunoprecipitated (IP) with anti-TRPC1 antibody or antibody preabsorbed with TRPC1 antigenic peptide. (**c**) Increase of surface TRPC1 by wild-type and $STIM1^{D76A}$ mutant but not $STIM1^{CT}$. (**d**) Coimmunoprecipitation of surface biotinylated TRPC1 with STIM1. (**e**) No effect of store depletion on the amount of surface TRPC1 that coimmunoprecipitates with STIM1. Cells were treated with 3 μM ionomycin or 2 μM thapsigargin for 15 min before lysis. (**f**) CFP–TRPC1 and YFP–STIM1 wild-type form punctae after store depletion. Note that both proteins colocalize well in resting cells and move from striped patterns to punctate locations after thapsigargin treatment. (**g**) Cocluster of CFP-tagged TRPC1 with YFP-tagged $STIM1^{D76A}$. (**f**, **g**) Live total internal reflection fluorescence images. The scale bars represent 10 μm.

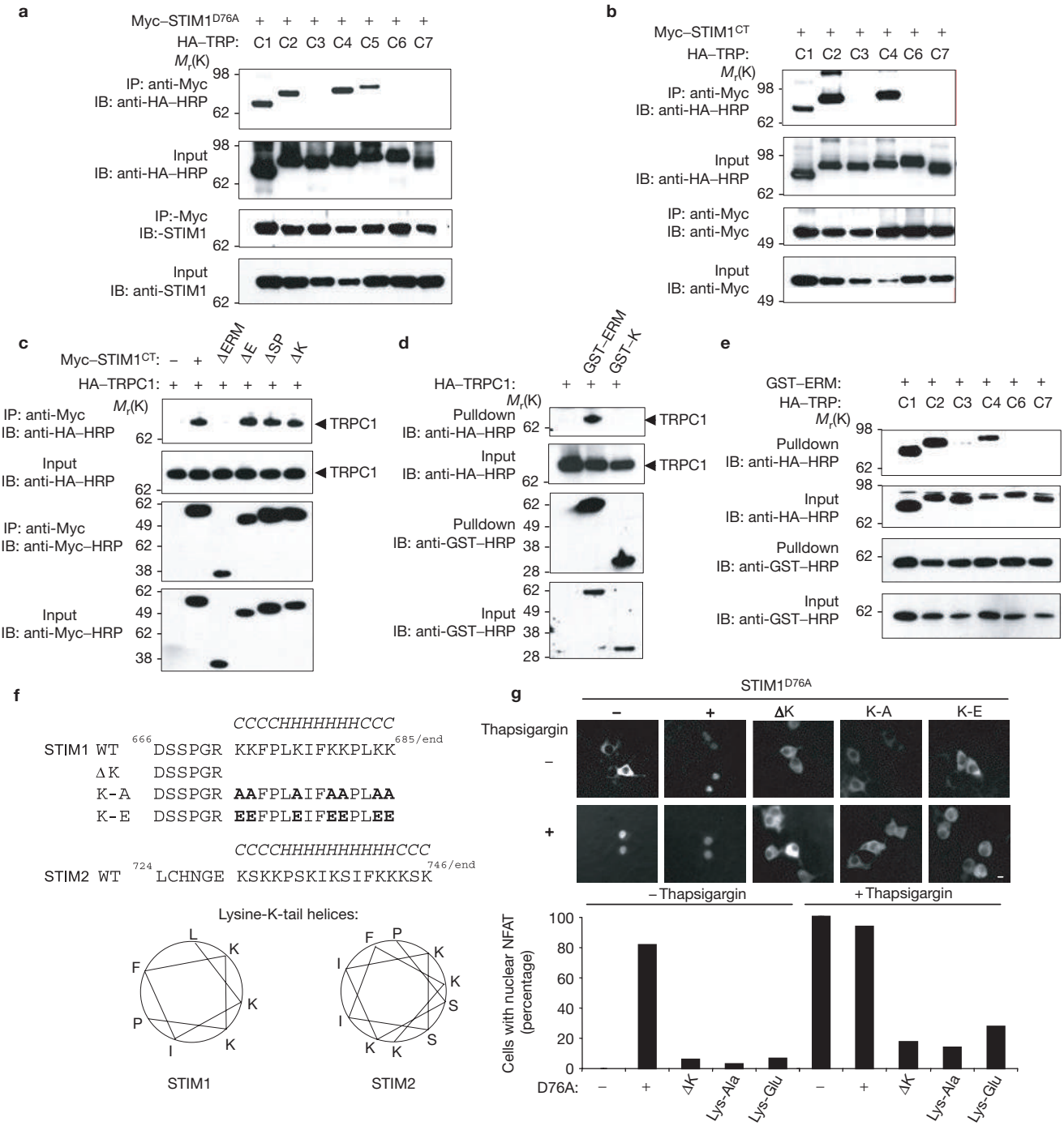

Figure 3 The ERM domain of STIM1 binds TRPC channels, and the cationic lysines in the lysine-rich tail are essential for SOC-channel activation. (**a**) Coimmunoprecipitation of STIM1^{D76A} with TRPC1, 2, 4 and 5, but not 3, 6 or 7 in HEK293 cells. (**b**) STIM1 cytosolic fragments are sufficient to coimmunoprecipitate with TRPC1, 2 and 4. (**c**) The ERM domain, but not glutamate-rich, serine–proline-rich or lysine-rich sequences of STIM1 are necessary for association with TRPC1. (**d**) The ERM domain is sufficient for binding to TRPC1. TRPC1 is coexpressed with GST–ERM or GST–lysine-rich tails in HEK293 cells and GST fusion protein is pulled down by glutathione beads. TRPC1 is only detected in the GST–ERM pulldown products. (**e**) GST–ERM confers binding selectivity with TRPC1, 2 and 4. TRPC5 did not express in these cotransfections. (**f**) Shown are the amino-acid sequences of STIM1 and STIM2 lysine-rich tails and corresponding mutations in the deletion and point mutants. The italic letters above the sequences indicate the secondary structure predicted by the Psi Predict programme (C, coil; H, helix). Below are the helical wheel representations of the amino acids in the middle helices of the STIM lysine-rich tails. (**g**) Images and summary of NFAT1–GFP localization in HEK293 cells coexpressing indicated STIM1^{D76A} proteins with different mutations in the lysine-rich tail before (–) or after (+) thapsigargin treatment. The scale bar represents 10 μm. Values are the means of results from triplicate wells. IB, immunoblot.

To determine the functional properties of STIM1 domains in Ca^{2+} influx, we monitored Ca^{2+} dynamics in HEK cells. Consistent with previous reports[3,4,6], overexpression of wild-type STIM1 had no effect on the spontaneous Ca^{2+} influx, but doubled the store-depletion-dependent Ba^{2+} influx, which is used as a Ca^{2+} surrogate to monitor unidirectional divalent ion influx by SOC channels (Fig. 1e). In contrast, STIM1^{D76A}

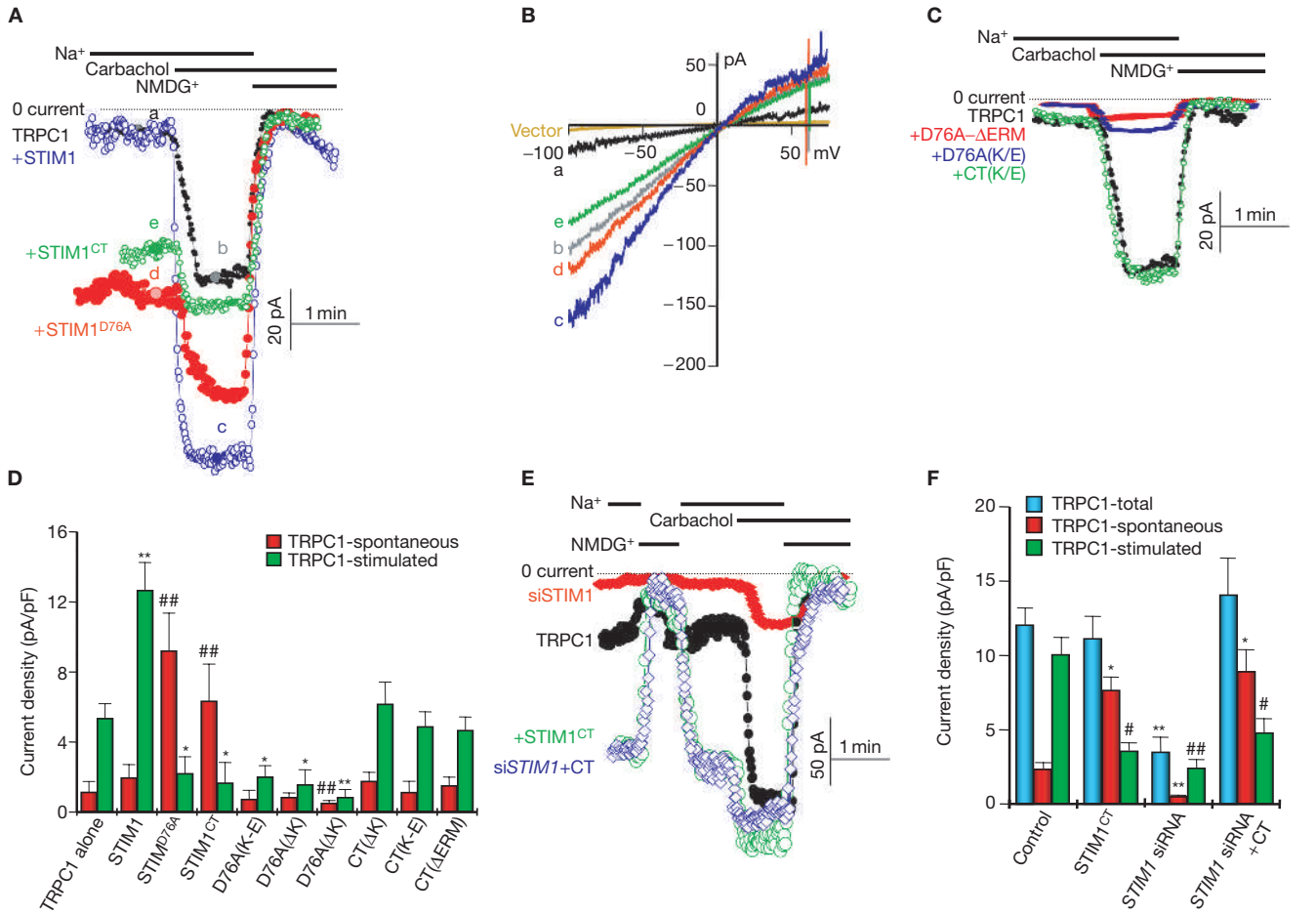

Figure 4 Effect of STIM1 constructs on TRPC1 activity. (**A**) HEK293 cells cotransfected with TRPC1 and GFP alone (black in **A** and **B**) or with STIM1 (blue), STIM1^{CT} (green) or STIM1^{D76A} (red) were used to measure TRPC1 currents before and after stimulation with 100 μM carbachol. (**B**) I/V curves obtained by –100 to +80 mV RAMPs with cells transfected with vector (brown) and the STIM1 constructs in **A**. a–e and the large symbols in **A** indicate the areas from where the I/Vs in **B** were taken. (**C**) As in **A**, except that the cells were cotransfected with TRPC1 and STIM1$^{D76A–ΔERM}$ (red), STIM1$^{D76A(K/E)}$ (blue) or STIM1$^{CT(K/E)}$ (green). (**D**) Spontaneous (red) and carbachol-stimulated (green) TRPC1 current with the indicated STIM1 constructs. (**E**, **F**) HEK cells were treated with scrambled (control) or *STIM1* siRNA and transfected with STIM1^{CT} and analysed for TRPC1 current (**E**). The summary in **F** is the mean ± s.e.m. of total (blue), spontaneous (red) and carbachol-activated (green) current density. The results are the mean ± s.e.m. (Control, $n=8$; STIM1^{CT}, $n=4$; *STIM1* siRNA, $n=6$; *STIM1* siRNA+CT, $n=6$). * and # denote $P < 0.05$ and ** and ## denote $P < 0.01$

increased resting intracellular $[Ca^{2+}]_i$ and store-depletion-dependent influx of Ba^{2+}. STIM1^{CT} also increased resting $[Ca^{2+}]_i$ and Ba^{2+} influx (Fig. 1e), supporting the notion that it directly activates the SOC channels. STIM1$^{D76A–ΔERM}$ reduces resting $[Ca^{2+}]_i$ and blocks Ba^{2+} influx, which is consistent with dominant-negative activity. Thus, Ca^{2+} measurements precisely match predictions from GFP–NFAT screening studies.

TRP channel family members have been implicated in the SOC channels of several cells, including HEK293 cells[11]. To examine whether TRPC channels are a target of STIM1, we assayed for their physical interaction. TRPC1 coimmunoprecipitates with STIM1 or STIM1^{D76A} when coexpressed in HEK293 cells (Fig. 2a). Moreover, native STIM1 coimmunoprecipitates with TRPC1 from the brain (Fig. 2b). Assays of surface-expressed TRPC1 and STIM1 indicate that both wild-type STIM1 and STIM1^{D76A}, but not STIM1^{CT}, produce an approximately 2–3-fold increase in surface expression of TRPC1 (Fig. 2c). Both wild-type STIM1 and STIM1^{D76A} are detected at the plasma membrane by surface biotinylation and are equally effective in the coimmunoprecipitation of TRPC1 (Fig. 2d). Store depletion with thapsigargin or ionomycin had no effect on the coimmunoprecipitation of TRPC1 with STIM1 (Fig. 2e), indicating that the physical interaction between the proteins, as assayed by coimmunoprecipitation, is not regulated by store depletion. In contrast, when HEK293 cells that coexpress CFP–TRPC1 and YFP–STIM1 are treated with thapsigargin, both proteins translocate within the cell and colocalize in punctae (Fig. 2f). CFP–TRPC1 also colocalizes with the constitutively active YFP–STIM1^{D76A} in discrete punctae that are evident in resting cells (Fig. 2g). These observations indicate that TRPC1 and STIM1 form a stable biochemical association and move together in the process of store-dependent punctae formation.

We examined the structural determinants of STIM1–TRPC1 interaction. STIM1^{D76A} coimmunoprecipitates TRPC1, 2, 4 and 5, which are implicated as SOC channels, but not TRPC3, 6 and 7 (Fig. 3a). STIM1^{CT} is sufficient to selectively coimmunoprecipitate TRPC family members (Fig. 3b), and the ERM domain is necessary and sufficient for selective coimmunoprecipitation with TRPC family members (Fig. 3c–e). In contrast, the lysine-rich region of STIM1 does not bind TRPC1 (Fig. 3c, d). The lysine-rich region contains 14 amino acids that are predicted to form

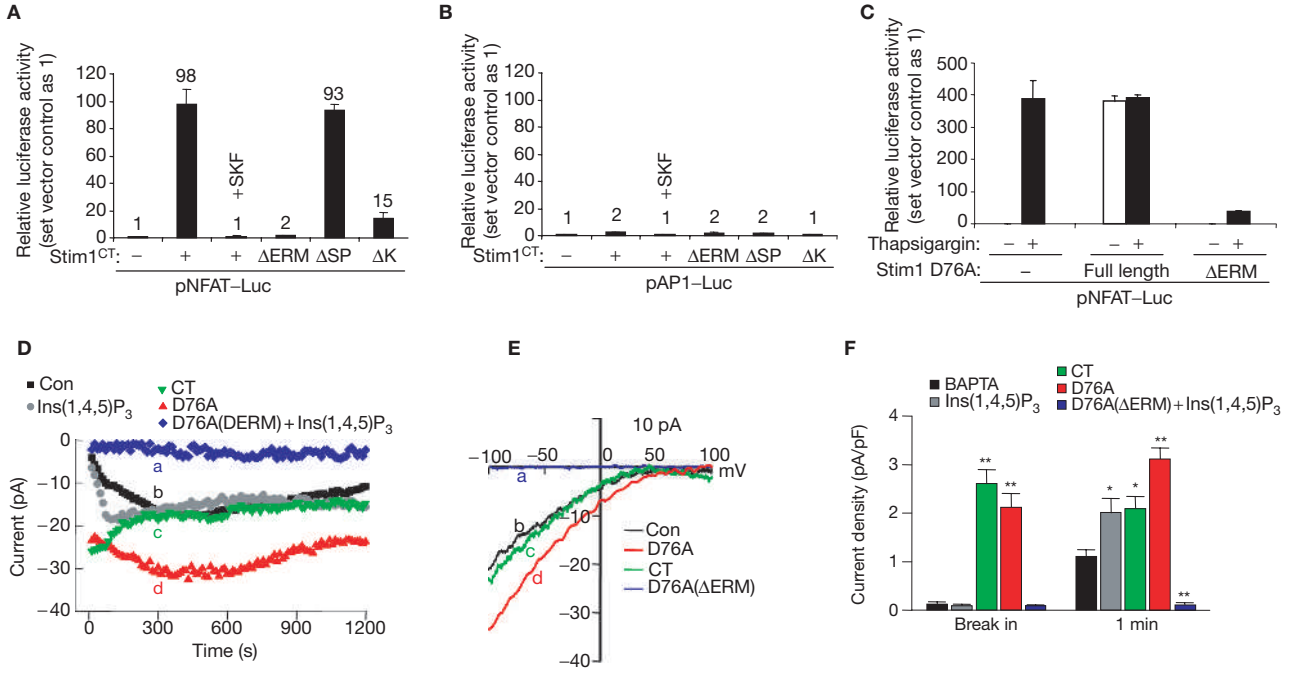

Figure 5 The STIM1^{D76A} full-length and the carboxyl terminus activate I_{crac} channels in Jurkat T cells, and require the ERM domain and the lysine-rich tail. (**A**, **B**) The NFAT-dependent (**A**) and the AP1-dependent (**B**) luciferase reporter expressions in Jurkat T cells transfected with indicated STIM1 cytosolic fragment constructs. (**C**) The effect of thapsigargin treatment and the expression of STIM1^{D76A} full-length or mutants lacking the ERM domain on the NFAT responsive expression of luciferase. Cells in **A**–**C** are all treated with phorbol myristate acetate (PMA). Error bars indicate s.e.m. (n=2). (**D**) Control (Con) Jurkat cells were dialyzed with a pipette solution containing 10 mM BAPTA that slowly depleted the stores to fully activate I_{crac} channels in about 5 min (black squares). Including 30 μM Ins (1,4,5)P_3 in the pipette solution accelerates I_{crac}-channel activation that was completed in 1 min (grey). Transfection of STIM1^{D76A} (red) or STIM1^{CT} (green) activated I_{crac} channels in the absence of Ca^{2+} store depletion. In cells transfected with STIM1$^{D76A-\Delta ERM}$, dialysed with 10 mM BAPTA and 30 μM Ins(1,4,5)P_3 and treated with 100 μM CPA. I_{crac} channels are completely inhibited. (**E**) Example of I/V curves recorded 5 min after establishing the whole-cell configuration and obtained from control cells (black) or cells transfected with the indicated STIM1 constructs. The letters **a**–**d** and the large symbols in **D** correspond to the traces in **E**. (**F**) Current recorded immediately after break-in and 1 min later in experiments similar to those in **D** and expressing the indicated STIM1 constructs is given as the mean ± s.e.m. (BAPTA and Ins(1,4,5)P_3, n=6; all others, n=4. * denotes $P < 0.05$ and ** denotes $P < 0.01$. SKF, SKF96365.

a two-turn helix that is flanked by two lysines on either side (Fig. 3f). A similar structure is predicted for STIM2 (Fig. 3f). To determine whether the lysine residues are critical, we generated mutants with all lysines in the last 14 amino acids, substituted with alanines (Lys-Ala) or glutamates (Lys-Glu). The Lys-Ala mutations are predicted to disrupt the middle helical structure, but Lys-Glu mutations are predicted to preserve the structure. STIM1^{D76A}, with either Lys-Ala or Lys-Glu mutations, does not drive GFP–NFAT into the nucleus and, furthermore, these mutants function as dominant-negatives to block NFAT translocation by store depletion (Fig. 3g).

To assess whether TRPC mimics the native SOC channels in response to STIM1, we monitored TRPC1-dependent currents in HEK cells that coexpressed STIM1 constructs. Spontaneous and agonist-activated currents were measured before and after cell stimulation with 1 mM carbachol. TRPC1 alone produces a carbachol-stimulated current with a reversal potential close to 0 mV with 140 mM pipette Cs^+ and 140 mM bath Na^+, confirming the non-selective cation permeability of TRPC1 (ref. 12). When coexpressed with STIM1, the current increases approximately twofold, which is consistent with biochemical data showing that STIM1 increases plasma-membrane expression of TRPC1 (Fig. 2c), but the current remains carbachol-dependent (Fig. 4A, B, D). In contrast, coexpression with STIM1^{D76A} results in a large spontaneous TRPC1-specific current that is only modestly increased by carbachol stimulation (Fig. 4A, B, D). A similar pattern of increased spontaneous and reduced carbachol-stimulated current is seen when TRPC1 is coexpressed with STIM1^{CT} (Fig. 4A, B, D). The effect of the STIM1^{CT} to increase spontaneous current is absent in mutants that lack the ERM or lysine-rich region, or in mutants that alter the charges of the lysine-rich region (Fig. 4C, D). Mutants that delete the ERM or modify the lysine-rich region from STIM1^{D76A} reduce both spontaneous and stimulated TRPC1 channel activity (Fig. 4C, D), which is consistent with dominant-negative activity. As anticipated from the binding data, STIM1^{CT} also activates TRPC4 (data not shown). These data indicate that STIM1 regulates TRPC1 and SOC channels in a similar manner, and support a model in which the C terminus of STIM1 regulates TRPC activity by a mechanism that involves ERM binding, and that requires the cationic lysine-rich region.

We examined whether STIM1^{CT} is sufficient to activate SOC and TRPC1 when native wild-type *STIM1* is knocked-down by small interfering RNA (siRNA) targeting an amino-terminal sequence and STIM1^{CT} is expressed alone or with TRPC1. *STIM1* siRNA effectively knocked-down native *STIM1* (see Supplementary Information, Fig. S3a) and eliminated the thapsigargin-stimulated NFAT translocation in HEK293 cells, which was fully restored by expression of STIM1^{CT} or STIM1^{CT} lacking the serine–proline-rich region but not the lysine-rich region (see Supplementary Information, Fig. S3b, c). Moreover, knockdown of *STIM1* blocked the activation of TRPC1 by carbachol (Fig. 4E, F), indicating that the native STIM1 is required for activation of TRPC1. Most notably, STIM1^{CT} rescued TRPC1 activity in siRNA-treated cells, and

most of the current was spontaneous, as found in control cells expressing TRPC1 and STIM1^{CT}. Similar effects were observed with SOC channels in HEK293 cells, measured as in Fig. 1e (data not shown).

In T cells, STIM1 also has an essential role in I_{crac}-mediated Ca^{2+} influx. Knockdowns of *STIM1* by siRNA markedly reduce I_{crac} currents that are activated by store depletion[3,5], and inhibit calcium influx in T cells[6]. To assess the functional properties of STIM1 constructs in T cells, we monitored NFAT responsive transcription of a luciferase reporter[13]. Expression of STIM1^{CT} increases luciferase activity by ~100-fold (Fig. 4A). The increase of luciferase activity is completely blocked by SKF96365, which indicates that the increased Ca^{2+} that activates the calcineurin–NFAT pathway enters through I_{crac} channels. A functional STIM1^{CT} in T cells requires both the ERM domain and the lysine-rich tail as deletion of either domain reduces luciferase expression by 50- and 6-fold, respectively (Fig. 5A). The NFAT-luciferase reporter[14] includes an AP1 site, and to confirm that this is not involved in activation by STIM1^{CT}, we determined that STIM1^{CT} has no effect on a specific AP1 reporter (Fig. 5B). STIM1^{D76A} activates luciferase expression to the same level as control cells treated with thapsigargin, and store depletion induces no further increase (Fig. 5C). In contrast, STIM1$^{D76A-\Delta ERM}$ does not activate the NFAT pathway, and reduces thapsigargin-dependent luciferase expression by 90% (Fig. 5C).

To directly examine the molecular mechanism of STIM1 in the regulation of I_{crac} channels, we measured I_{crac} current in Jurkat cells. Figure 5D shows the time dependence of I_{crac}-channel activation by patch recording with an internal buffer that includes BAPTA to deplete stores. Current/voltage (I/V) curves that were obtained 5 min after establishing the whole-cell configuration illustrate characteristic inward rectification (Fig. 5E). STIM1^{D76A} and STIM1^{CT} equally activate the I_{crac} current, as measured at break-in. As anticipated, STIM1$^{D76A-\Delta ERM}$ strongly inhibits I_{crac} even when Ins(1,4,5)P_3 is included in the pipette and the cells are treated with the SERCA inhibitor CPA.

The present study supports a model in which STIM1 activates SOC, I_{crac} and TRPC channels by a mechanism that involves ERM-dependent binding and lysine-rich-region-dependent activation of the channel from its position within the endoplasmic reticulum. If behaving similarly to TRPC1, the channels are constitutively bound to STIM1, and biochemically assayed binding is not regulated by store depletion. Ca^{2+} depletion leads to the translocation and co-clustering of the proteins at sites of close apposition between the plasma membrane and the endoplasmic reticulum, and promotes the action of the lysine-rich-region of STIM1 to affect channel opening. Although STIM1 is detected at the plasma membrane in both the resting and store-depleted state by surface biotinylation assays, this is not sufficient to open channels, indicating that clustering of STIM1 within the endoplasmic reticulum near the membrane that occurs with store depletion is the critical event for channel opening. The EF hand domain of STIM1, which resides within the endoplasmic reticulum, senses Ca^{2+} concentration and functions to inhibit STIM1 activity when stores are filled. STIM1^{CT} is constitutively active as it lacks the regulation that is afforded by the endoplasmic reticulum sensor. Both the ERM domain and the lysine-rich tail of STIM1 are crucial for the activation of endogenous SOC, I_{crac} and TRPC channels. The dominant-negative activity of STIM1$^{D76A-\Delta ERM}$ and STIM1$^{D76A-\Delta K}$ is not due to the inhibition of TRPC1 trafficking to the plasma membrane (see Supplementary Information, Fig. S4F). Rather, the dominant-negative activity of STIM1$^{D76A-\Delta ERM}$ seems to involve the inhibition of store-depletion-dependent clustering of wild-type STIM1 (see Supplementary Information, Fig. S4D), combined with its inability to bind and activate TRPC1. STIM1$^{D76A-\Delta K}$ does not interfere with wild-type STIM1 clustering (see Supplementary Information, Fig. S4E), but probably 'dilutes' the lysine-rich regions of native STIM1. Our data indicate that the lysine-rich region is effective when it is presented from a cytoplasmic source. Interestingly, the lysine-rich tail is not found in fly or worm STIM1 but is conserved in all vertebrate STIM homologues, indicating that the lysine-rich-region-dependent regulation of SOC channels is a vertebrate adaptation. We speculate that the positive charges in the STIM1 lysine-rich region interact with anionic lipids in the membrane or residues in other proteins to facilitate SOC- and I_{crac}-channel activation.

Previous studies have indicated a role for STIM1 at the plasma membrane in activating SOC channels. For example, extracellularly applied antibody to STIM1 was reported to reduce whole-cell current, but not unitary conductance of I_{crac} channels[3]. However, the mechanism of this effect was not determined. Consistent with a role for STIM1 at the plasma membrane, our findings indicate that STIM1 produces a modest increase of TRPC1 expression on the plasma membrane (Fig. 2c), and a comparable increase in the amplitude of the native SOC channels in HEK cells (Fig. 4) and I_{crac} in Jurkat cells (Fig. 5E), and may stabilize the channel at this location. However, the action of STIM1 to increase plasma-membrane channel expression is similar for STIM1 and STIM1^{D76A}, and is not seen with STIM1^{CT}, and therefore is not related to the ability of STIM1 to activate these channels. Indeed, knockdown of *STIM1* abolishes SOC/I_{crac} channels, but does not inhibit the ability of STIM1^{CT} to activate the channels. The present study highlights the essential functions of STIM1 for activation of membrane ion channels. □

METHODS

Cell culture and reagents. HEK293 cells (ATCC) were maintained in DMEM supplemented with 10% fetal bovine serum (FBS). Jurkat T cells were obtained from J. Liu (Johns Hopkins School of Medicine, Baltimore, MD) and grown in RPMI 1640 medium supplemented with 10% FBS. Reagents and sources included thapsigargin (2 μM, Calbiochem, San Diego, CA), CPA, Ins(1,4,5)P_3 (Alomone, Jerusalem, Israel), ionomycin (3 μM, Calbiochem), FK506 (0.1 μM, Sequoia Research Products, Pangbourne, UK), SKF 96365 (50 μM, Tocris, Ellisville, MI), PMA (50 ng ml^{-1}, Sigma, St Louis, MO), dithiobis(succinimidylpropionate) (DSP; Pierce, Rockford, IL), biotinylation reagent sulfo-NHS-SS-biotin (Pierce), neutroavidin beads (Pierce), anti-human STIM1 amino-terminus antibody (Pharmingen, San Diego, CA), horseradish peroxidase (HRP)-conjugated anti-GST antibody (Sigma), HRP-conjugated anti-HA antibody (Roche, Nutley, NJ), HRP-conjugated anti-Myc antibody (Santa Cruz Biotechnology, Santa Cruz, CA), anti-Myc antibody (Roche), anti-TRPC1 antibody (Alomone) and siRNA targeting human *Stim1-1140* (Dharmacon, Chicago, IL)[5].

Cloning and mutagenesis. Full-length *STIM1* was generated by polymerase chain reaction (PCR) using Jurkat T cell mRNA reverse-transcription product as template. A Myc tag (EQKLISEEDLNGGGGG) was inserted after the signal peptide cleavage site and between Ser 28 and Glu 29. The Motif Scan (www.scansit.mit.edu) and NCBI protein database (using Q13586 as entry) were used to predict the STIM1 domains and regions and their boundaries. The secondary structure of the lysine-rich tail of STIM1 was predicted by the PsiPredict program (at the expasy website; www.expasy.org). The cytosolic fragment of STIM1 was produced by PCR and subcloned into pRK5 after a Myc tag. All the deletion and point mutations were generated by PCR mutagenesis (Stratagene, La Jolla, CA). The deletion mutant ΔERM deletes 251–535, ΔE deletes 270–336, ΔSP deletes 600–629 and ΔK deletes 672–685. The GST–ERM and GST–lysine-rich tail were generated by subcloning the STIM1 244–542 and 672–685 PCR products into an eukaryotic GST expression vector (pCMV–GST)[15]. CFP–TRPC1 was generated by insertion of CFP into pRK5–HA–TRPC1 between HA and TRPC1. All constructs were confirmed by sequencing and protein expression was confirmed by western blot analysis.

Transfection and reporter assays. HEK293 cells were transfected using FuGene 6 (Roche) following the manufacturers' protocol. The localization of NFAT1–GFP was examined and scored in live cells overnight until 48 h after transfection. Cells were pretreated with FK506 or SKF for 15–30 min before stimulation or scoring, and thapsigargain or ionomycin was added 0.5–2 h before imaging of NFAT1–GFP. Jurkat T cells were transfected by electroporation[16]. The β-galatosidase expression plasmids were cotransfected with luciferase expression plasmids for normalization. After transfection (48 h), cells were treated with PMA (and thapsigargin) for 8 h. The luciferase and β-galatosidase activities were measured using luciferin (Promega, Madison, WI) and o-Nitrophenyl-β-D-galactopyranoside (ONPG; Sigma) as substrates, respectively[16].

Coimmunoprecipitation and pulldown assays. TRPC expression constructs and binding assays were described previously[17]. When coexpressed with $STIM1^{CT}$ or GST–ERM, TRPC5 did not express well (approximately fivefold less compared with other TRPCs), so the TRPC5 coimmunoprecipitation data is not included in Fig. 2b, e. For the brain coimmunoprecipitation of STIM1 and TRPC1, the cortex and hippocampus from an adult rat were homogenized with a buffer containing 13% sucrose, 0.2 mM HEPES at pH 7.4, 5 mM EDTA, 0.2 mM PMSF and one protease inhibitor tablet (Roche). After centrifugation at 800*g* for 15 min, the supernatant was further spun at 9,200*g* for 15 min. The pellet after the second centrifugation is the membrane (P2) faction[18]. The membrane pellet was solubilized with immunoprecipitation buffer containing 2.5 mg ml^{-1} DSP and 1% Triton X-100. After termination of the crosslinking reaction, the solubilized fraction was subjected to regular immunoprecipitation procedures[17] with anti-TRPC1 antibody or antibody premixed with the TRPC1 antigen peptide at 4 °C overnight (preabsorbed). For the detection of surface protein, cells expressing the indicated proteins were surface biotinylated and lysed in 1% SDS containing buffer. The biotinylated proteins were pulled down by neutroavidin beads and loaded for western blot analysis. For coimmunoprecipitation of surface TRPC1 with STIM1, cells were treated as indicated in complete culture medium (including 2 mM Ca^{2+}) and then surface biotinylated at 4 °C for 30 min. Cells were lysed in 1% Triton X-100 containing immunoprecipitation buffer and the STIM1-interacting proteins were immunoprecipitated. The bound proteins were eluted with phosphate-buffered saline–1% SDS and the eluates were further pulled down by neutroavidin beads with 1% SDS in all buffers for incubation and washing. This two-step procedure allows the isolation of STIM1 binding proteins that are biotinylated on the cell surface.

Measurement of $[Ca^{2+}]_i$. HEK293 cells were loaded with Fura 2 and the 340:380 ratio was measured as described previously[17]. During fluorescence measurements, the cells were continually perfused with a bath solution (37 °C) containing 150 mM NaCl, 5 mM KCl, 1 mM $MgCl_2$, 10 mM glucose, 10 mM HEPES at pH 7.4 with NaOH, and either 1 mM $CaCl_2$, 2 mM Ba^{2+} or 0.5 mM EGTA (Ca^{2+}-free).

Cell imaging. HEK293 cells were plated on poly-L-ornithine-coated petri dishes, each with a coverslip attached to the bottom. Cells were cotransfected with CFP-tagged TRPC1 and YFP-tagged STIM1 using FuGene 6 (Roche). One day after transfection, live cells were imaged using a total internal reflection fluorescence microscope with a 60× objective.

Current measurement in HEK293 and Jurkat cells. TRPC1 current in HEK293 cells was measured as described previously[17] with a pipette solution composed of 140 mM CsCl, 2 mM $MgCl_2$, 1 mM ATP, 5 mM EGTA and 10 mM HEPES at pH 7.2 with Tris-base, and a bath solution containing either 140 mM NaCl or 140 mM NMDG-Cl, 5 mM KCl, 0.5 mM EGTA and 10 mM HEPES at pH 7.4 with NaOH or NMDG-OH. TRPC1 current was recorded by stepping up the membrane potential to −80 mV for 200 msec every 6 s from a holding membrane potential of 0 mV or by 400 msec rapid alteration of membrane potentials (RAMPs) from −100 to +80 mV from a holding potential of 0 mV. The current at −80 mV was used to calculate current density. Ca^{2+} current by I_{crac} channels in Jurkat cells was isolated as described previously[19] using a pipette solution containing 140 mM Cs^+-Glutamate, 1 mM ATP, 8 mM $MgCl_2$ (to inhibit MIC–TRPM7), 10 mM BAPTA and 10 mM HEPES (pH 7.2 with CsOH). The bath solution contained 150 mM NMDG–gluconate, 10 mM HEPES at pH 7.4 with Tris or the same solution in which 20 mM $CaCl_2$ replaced 30 mM NMDG–gluconate. The cells were held at 0 mV and Ca^{2+} current was measured by delivering RAMPs from −100 to +100 mV for 400 msec every 6 s. The current measured on break-in was used for leak current subtraction for all STIM1 constructs except for $STIM1^{CT}$ and $STIM1^{D76A}$, in which case the current recorded on break-in in control cells was used.

Accession numbers. The ERM domain of human STIM1 (Q13586: 251–535 amino acids) was used for a BLAST NCBI search and the following homologous sequences were found and aligned in Supplementary Information Fig. S2: *Caenorhabditis elegans* (AAF59596.3: 209–387 amino acids), *Apis mellifera* (XP_395207.2: 279–469 amino acids), *Drosophila melanogaster* (AAK82338.1: 331–553 amino acids), *Danio rerio* (XP_684241.1: 245–519 amino acids), *Tetraodon nigroviridis* (CAG08997.1: 152–446 amino acids), *Xenopus tropicalis* (AAH66133.1: 240–513 amino acids), *Gallus gallus* (CAG32447.1: 177–460 amino acids), *Canis familiaris* (XP_862122.1: 251–535 amino acids), *Bos taurus* (NP_001030486.1: 249–533 amino acids), *Mus musculus* (AAH21644.1: 251–535 amino acids), *Rattus. norvegicus* (XP_341897.2: 251–535 amino acids), *Pan troglodytes* (XP_508237.1: 224–539 amino acids).

Note: Supplementary Information is available on the Nature Cell Biology website.

ACKNOWLEDGEMENTS

We thank J. Liu (Johns Hopkins University) for the plasmids NFAT1–GFP (HA–mNFAT1(1–460)–GFP), pNFAT-luc, pAP1-luc and pSV40-β-galactosidase; and T. Meyer (Stanford University) for the plasmid YFP–STIM1. Research was supported by grants from the National Institute on Drug Abuse (NIDA; DA00266, DA10309) and the National Institute of Mental Health (NIMH; MH068830) to P.F.W., and the National Institute of Dental and Craniofacial Research (NIDCR) and National Institute of Diabetes, Digestive and Kidney Diseases (NIDDK) to S.M.

COMPETING FINANCIAL INTERESTS

The authors declare that they have no competing financial interests.

Published online at http://www.nature.com/naturecellbiology/
Reprints and permissions information is available online at http://npg.nature.com/reprintsandpermissions/

1. Parekh, A. B. & Putney, J. W., Jr. Store-operated calcium channels. *Physiol. Rev.* **85,** 757–810 (2005).
2. Berridge, M. J., Bootman, M. D. & Roderick, H. L. Calcium signalling: dynamics, homeostasis and remodelling. *Nature Rev. Mol. Cell Biol.* **4,** 517–529 (2003).
3. Spassova, M. A. *et al.* STIM1 has a plasma membrane role in the activation of store-operated Ca^{2+} channels. *Proc. Natl Acad. Sci. USA* **103,** 4040–4045 (2006).
4. Zhang, S. L. *et al.* STIM1 is a Ca^{2+} sensor that activates CRAC channels and migrates from the Ca^{2+} store to the plasma membrane. *Nature* **437,** 902–905 (2005).
5. Roos, J. *et al.* STIM1, an essential and conserved component of store-operated Ca^{2+} channel function. *J. Cell Biol.* **169,** 435–445 (2005).
6. Liou, J. *et al.* STIM is a Ca^{2+} sensor essential for Ca^{2+}-store-depletion-triggered Ca^{2+} influx. *Curr. Biol.* **15,** 1235–1241 (2005).
7. Feske, S. *et al.* A mutation in Orai1 causes immune deficiency by abrogating CRAC channel function. *Nature* **441,** 179–186 (2006).
8. Vig, M. *et al.* CRACM1 is a plasma membrane protein essential for store-operated Ca^{2+} entry. *Science* **312,** 1220–1223 (2006).
9. Williams, R. T. *et al.* Identification and characterization of the STIM (stromal interaction molecule) gene family: coding for a novel class of transmembrane proteins. *Biochem. J.* **357,** 673–685 (2001).
10. Crabtree, G. R. & Olson, E. N. NFAT signaling: choreographing the social lives of cells. *Cell* **109** (Suppl.), S67–S79 (2002).
11. Freichel, M. *et al.* Functional role of TRPC proteins in native systems: implications from knockout and knock-down studies. *J. Physiol.* **567,** 59–66 (2005).
12. Lintschinger, B. *et al.* Coassembly of Trp1 and Trp3 proteins generates diacylglycerol- and Ca^{2+}-sensitive cation channels. *J. Biol. Chem.* **275,** 27799–27805 (2000).
13. Northrop, J. P., Ullman, K. S. & Crabtree, G. R. Characterization of the nuclear and cytoplasmic components of the lymphoid-specific nuclear factor of activated T cells (NFAT) complex. *J. Biol. Chem.* **268,** 2917–2923 (1993).
14. Northrop, J. P. *et al.* NFAT components define a family of transcription factors targeted in T-cell activation. *Nature* **369,** 497–502 (1994).
15. Tsai, R. Y. & Reed, R. R. Using a eukaryotic GST fusion vector for proteins difficult to express in *E. coli*. *Biotechniques* **23,** 794–796, 798, 800 (1997).
16. Sun, L. *et al.* Cabin 1, a negative regulator for calcineurin signaling in T lymphocytes. *Immunity* **8,** 703–711 (1998).
17. Yuan, J. P. *et al.* Homer binds TRPC family channels and is required for gating of TRPC1 by IP3 receptors. *Cell* **114,** 777–789 (2003).
18. Xiao, B. *et al.* Homer regulates the association of group 1 metabotropic glutamate receptors with multivalent complexes of homer-related, synaptic proteins. *Neuron* **21,** 707–716 (1998).
19. Kozak, J. A., Kerschbaum, H. H. & Cahalan, M. D. Distinct properties of CRAC and MIC channels in RBL cells. *J. Gen. Physiol.* **120,** 221–235 (2002).

nature cell biology

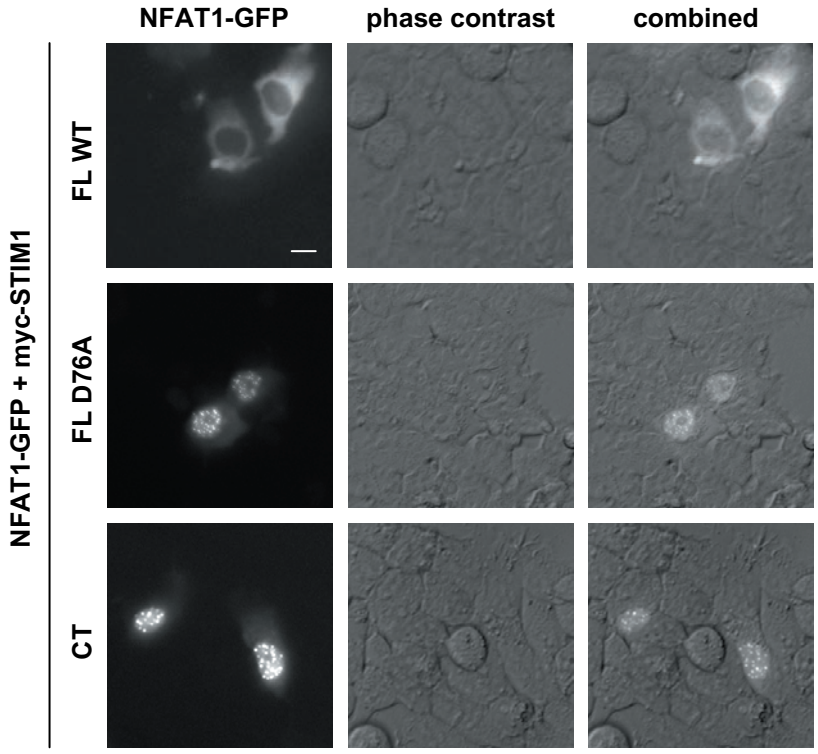

Figure S1 Fluorescence and phase contrast images of cells expressing NFAT-GFP. Note cytosolic and intranuclear localizations of GFP-NFAT. Scale bar, 10 um.

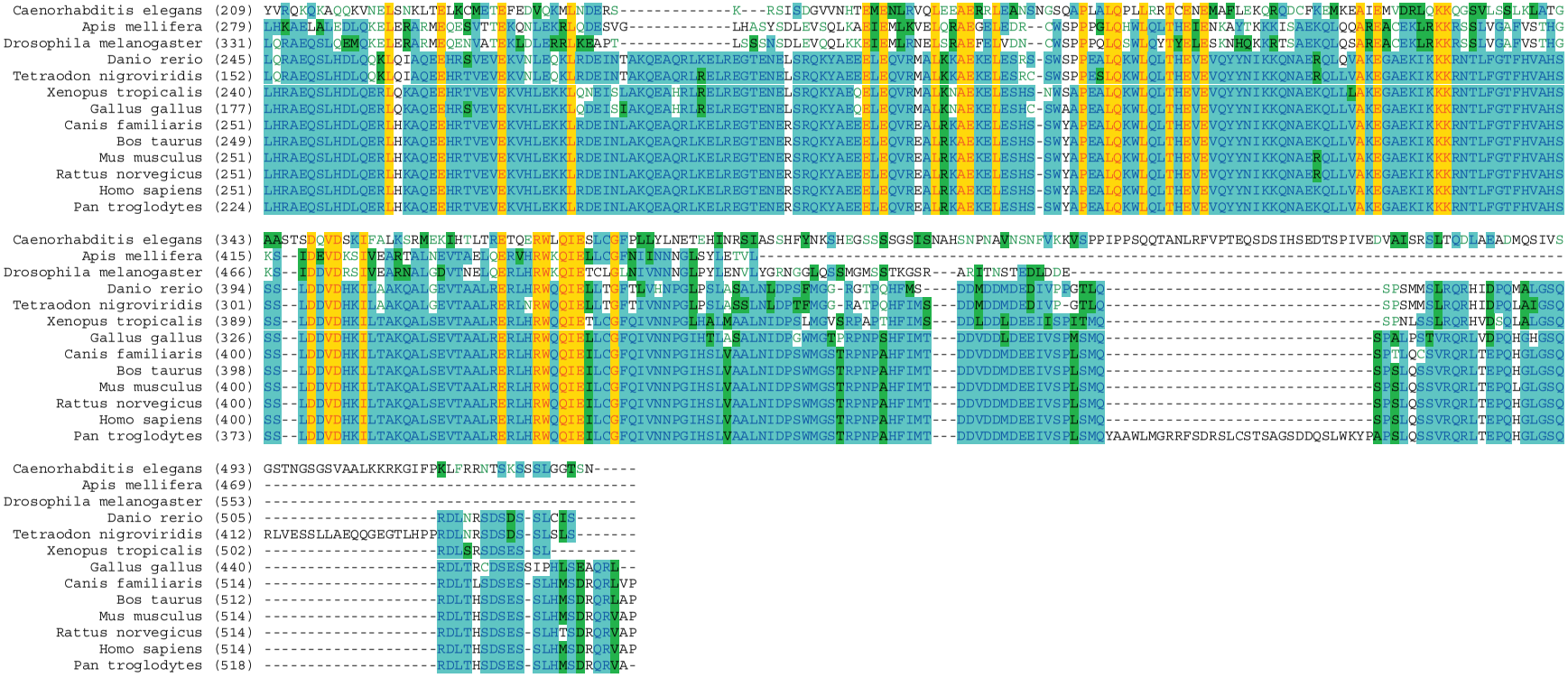

Figure S2 Sequence alignment of ERM domain of STIM homologs. Shown is the alignment of the ERM domain sequences from difference species. The amino acids identical in all species are in yellow and those identical in most species are in blue, and the similar amino acids are shown in green.

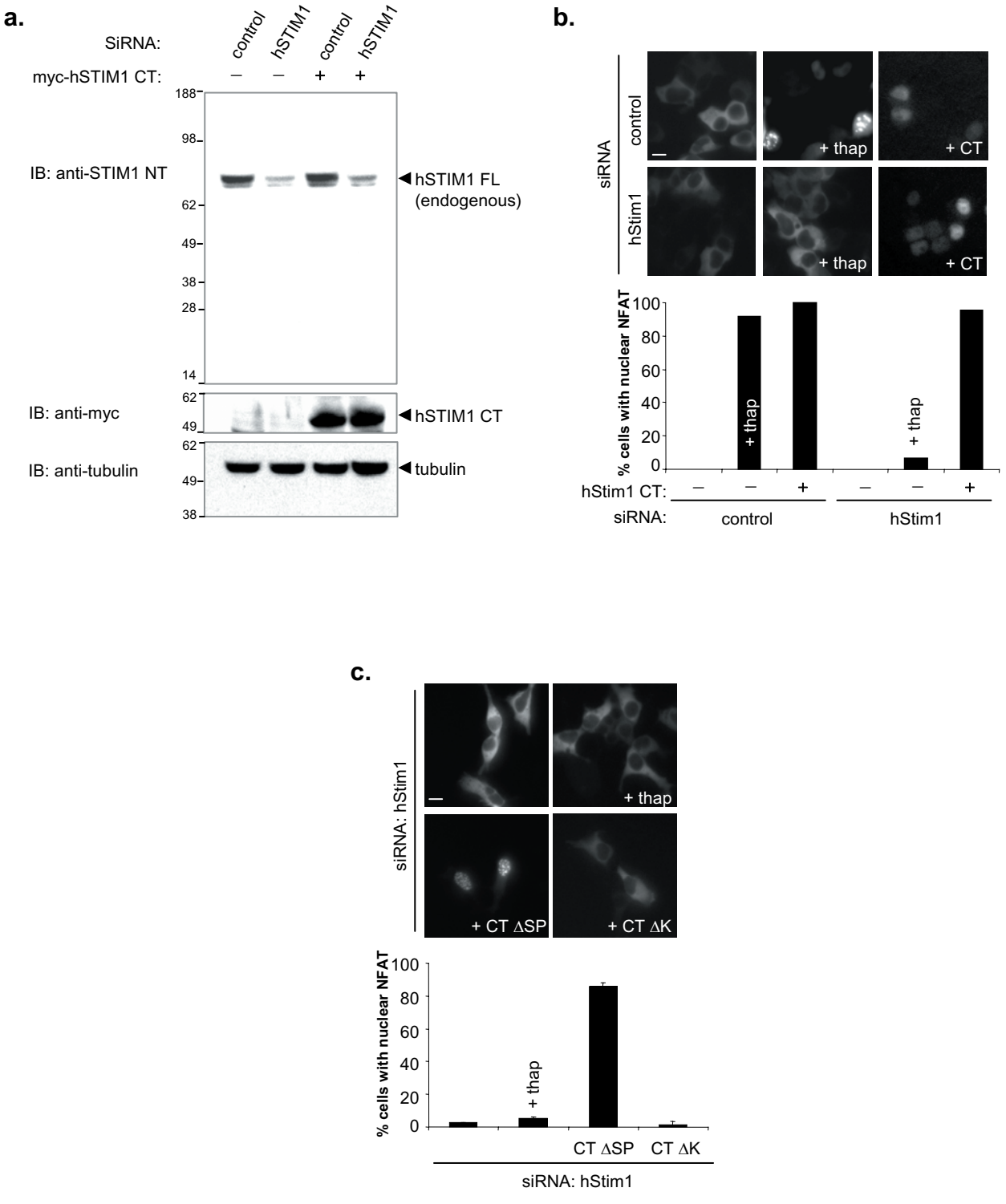

Figure S3 Knockdown of STIM1 does not alter activity of STIM1-CT. HEK cells were treated with scrambled (control) or STIM1 siRNA and transfected with STIM1 C- term and analyzed for expression of STIM1 and STIM1 C-term **(a)** and GFP-NFAT translocation **(b, c).** Scale bar, 10 um.

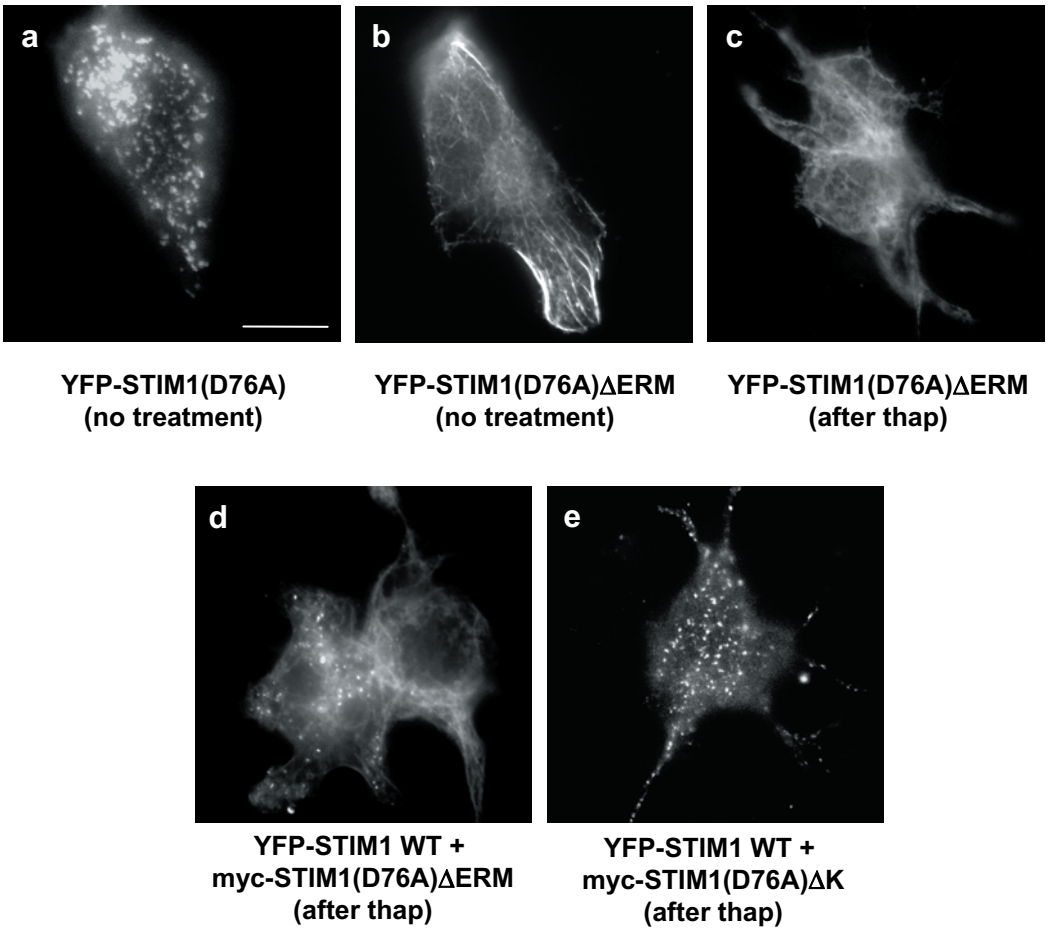

Figure S4 STIM1(D76A)ΔERM blocks clustering of wt STIM1. The ERM domain-deficient STIM1(D76A)ΔERM mutant does not form punctae **(b, c)** and appears to block the translocation and clustering of wild type STIM1 upon store depletion **(d)**, but STIM1(D76A)ΔK does not block **(e)**. In d, two cells with one showing partial (left) and the other showing complete (right) block of STIM1 clustering in response to thapsigargin are presented. All images are live epi-fluorescence images. Scale bar, 10 um. f. WT and D76A mutant STIM1 but not the STIM1 C-terminus increase surface TRPC1, while STIM1 dominant negatives don't block TRPC1 surface trafficking.